

Plasma Catalysis Modelling: How Ideal is Atomic Hydrogen for Eley-Rideal?

Roel Michiels^a, Nick Gerrits^{a,b,*}, Erik Neyts^a and Annemie Bogaerts^{a,+}

^a Research group PLASMANT, Department of Chemistry, University of Antwerp, Universiteitsplein 1, BE-2610 Wilrijk-Antwerp, Belgium

^b Leiden Institute of Chemistry, Gorlaeus Laboratories, Leiden University, P.O. Box 9502, 2300 RA Leiden, The Netherlands

*: n.gerrits@lic.leidenuniv.nl, +31715271328

+: annemie.bogaerts@uantwerpen.be, +3232652377

S.1 Convergence of computational parameters for DFT calculations

The adsorption energy of species, E_{ads} , is defined as:

$$E_{ads} = E_{adsorbate+surface} - (E_{surface} + E_{adsorbate})$$

Where $E_{adsorbate+surface}$, $E_{surface}$, and $E_{adsorbate}$ are the total energies of the adsorbate on the slab, the clean slab and the gaseous adsorbate, respectively.

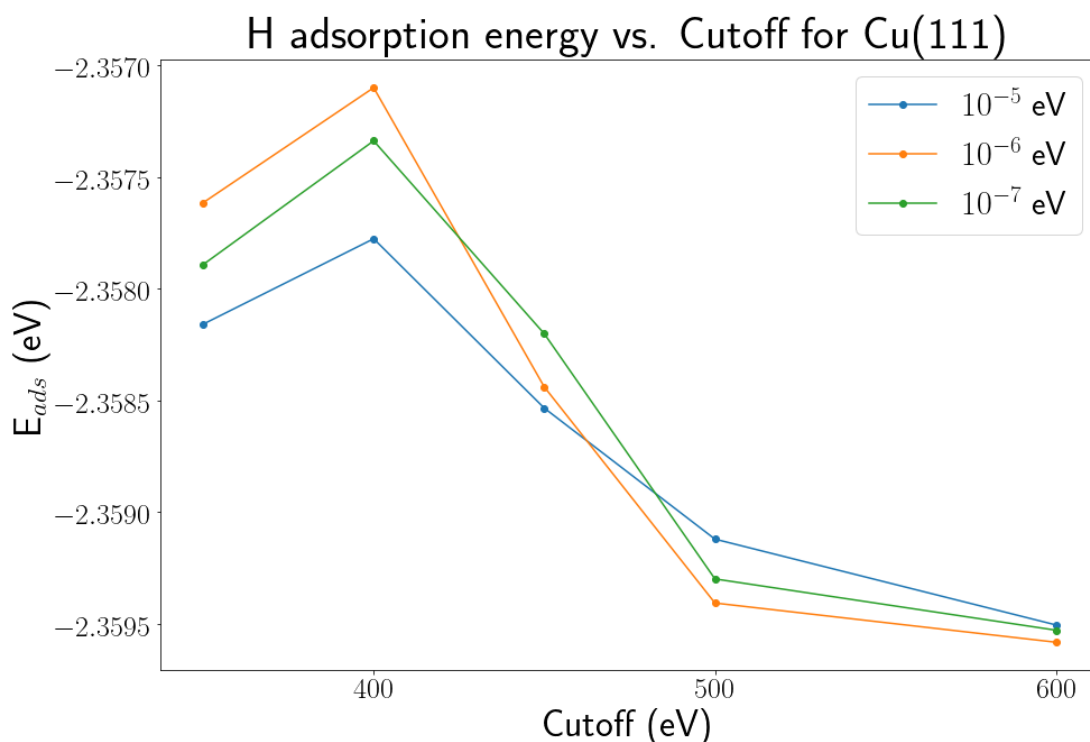


Figure S1: Convergence of the H adsorption energy on Cu(111) as a function of the cutoff. The different lines show the convergence for different electronic SCF convergence criteria.

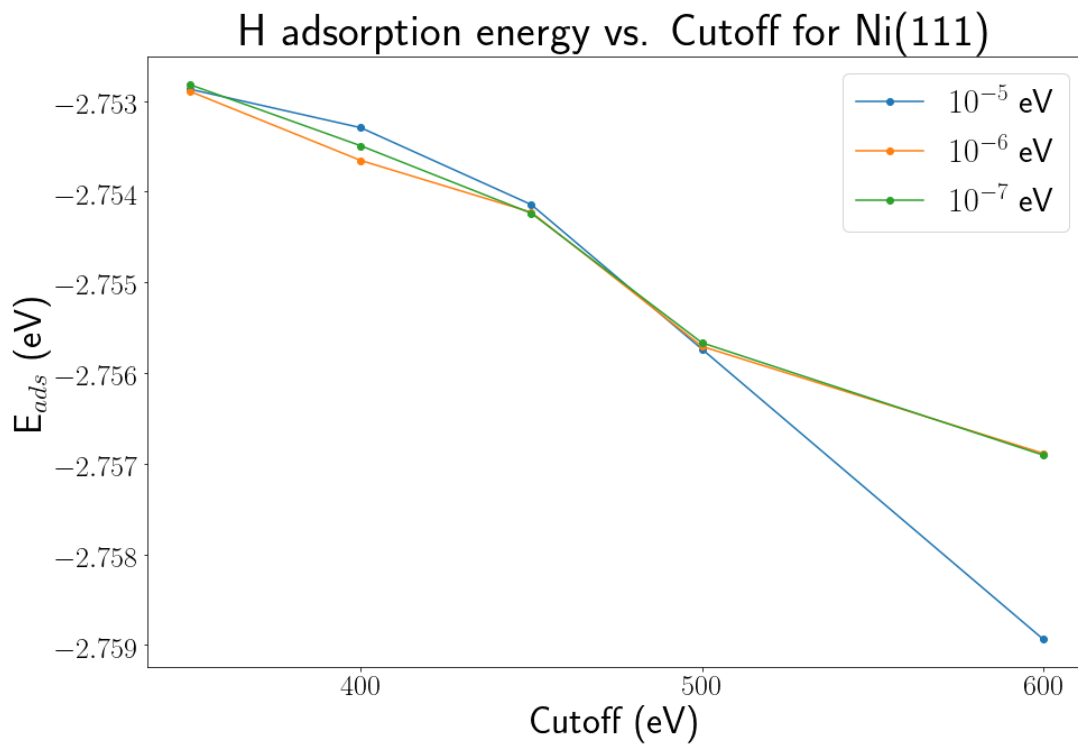


Figure S2: Convergence of the H adsorption energy on Ni(111) as a function of the cutoff. The different lines show the convergence for different electronic SCF convergence criteria.

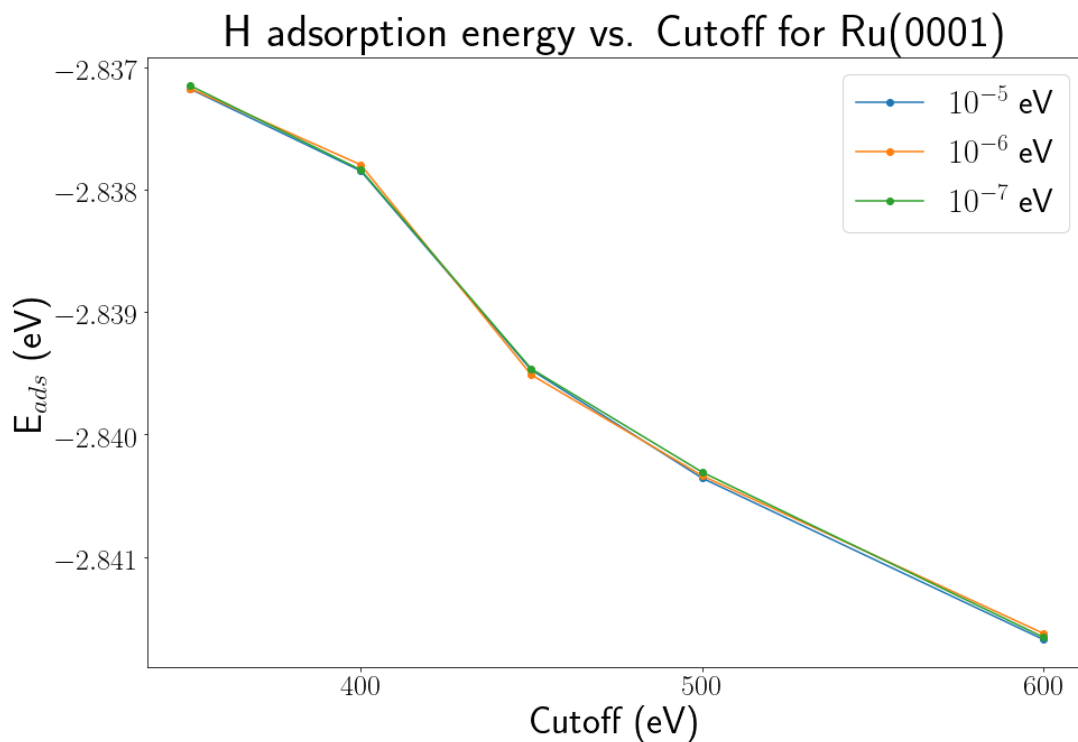


Figure S3: Convergence of the H adsorption energy on Ru(0001) as a function of the cutoff. The different lines show the convergence for different electronic SCF convergence criteria.

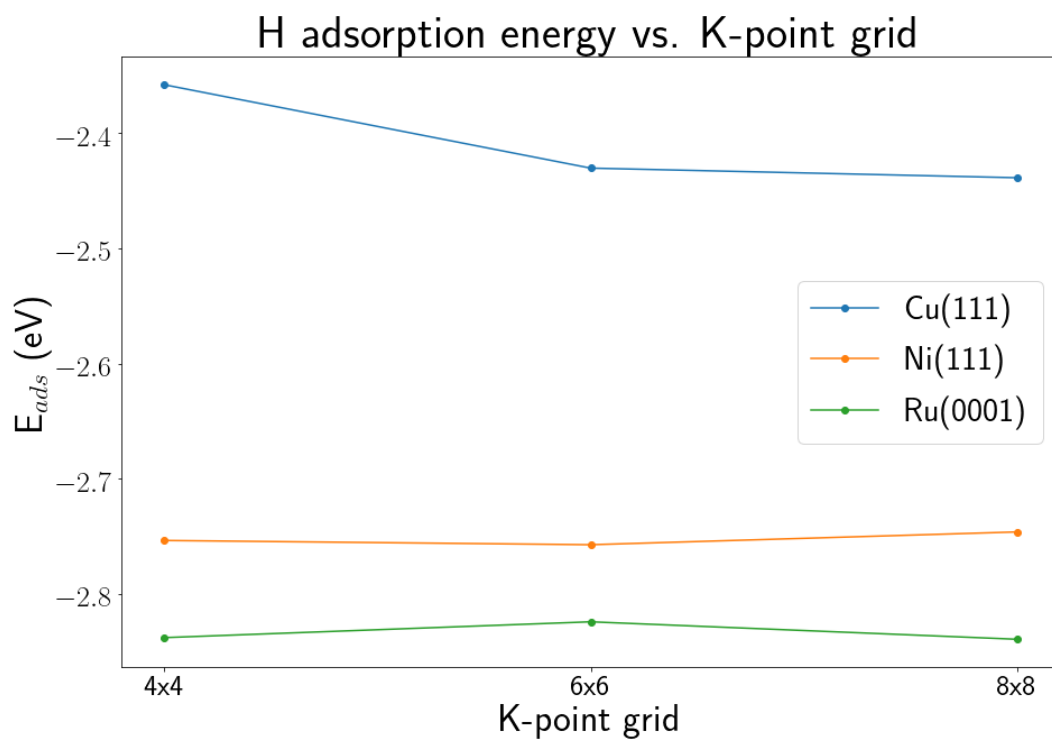


Figure S4: Convergence of the H adsorption energy as a function of the K-point grid. The different lines show the convergence for different metals.

S.2 PES intersections

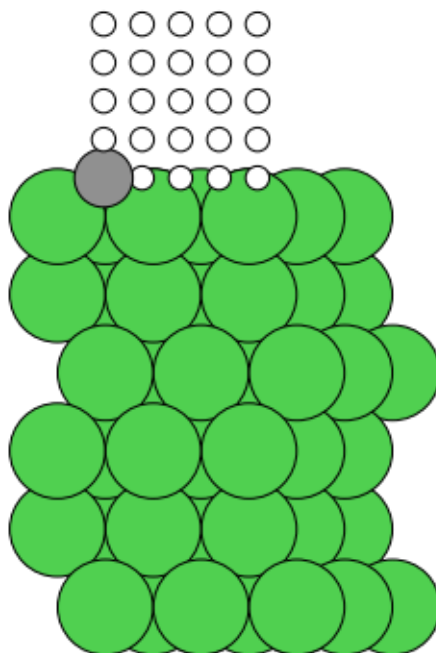


Figure S.5: Illustrative picture on how the PES intersections are constructed for $H(g) + C^*$ at Ni(111). The distance between the H atom positions is not to scale. The different positions of the H atom are represented by white spheres.

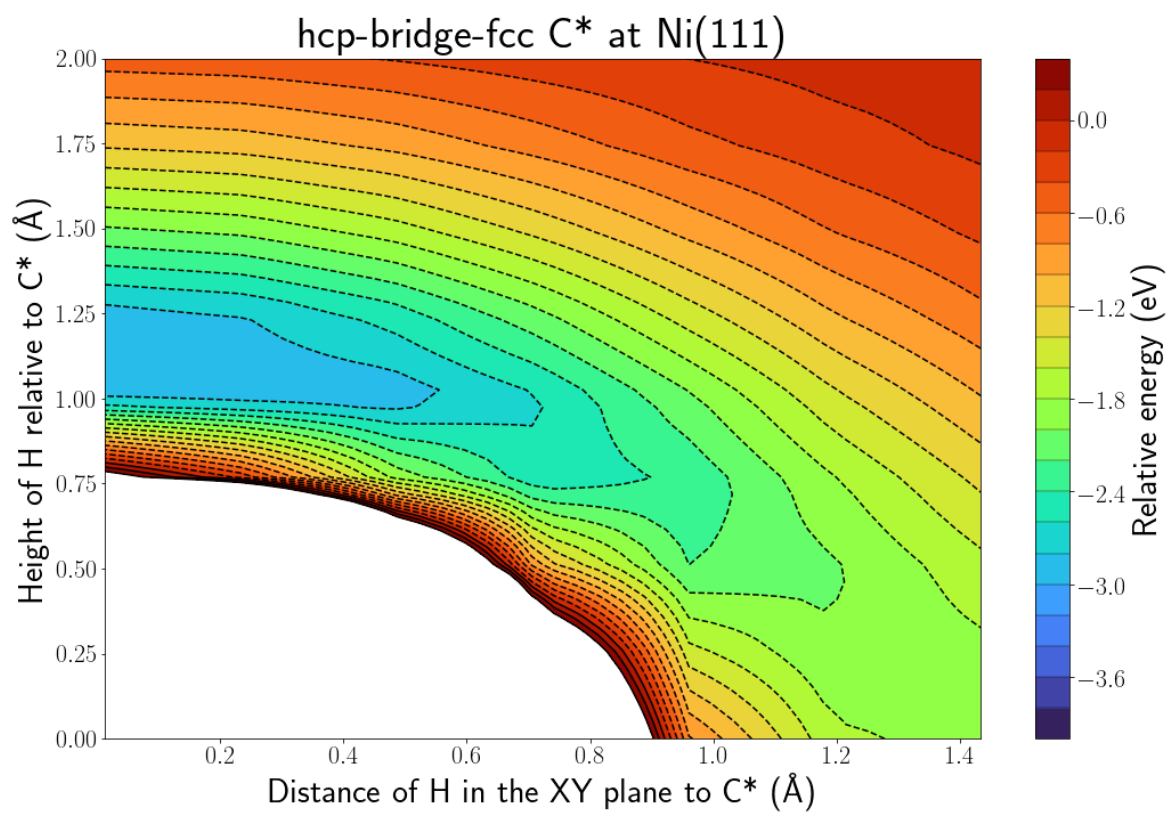


Figure S.6: PES intersection for H(g) + C* at Ni(111) surface along the hcp-bridge fcc line.

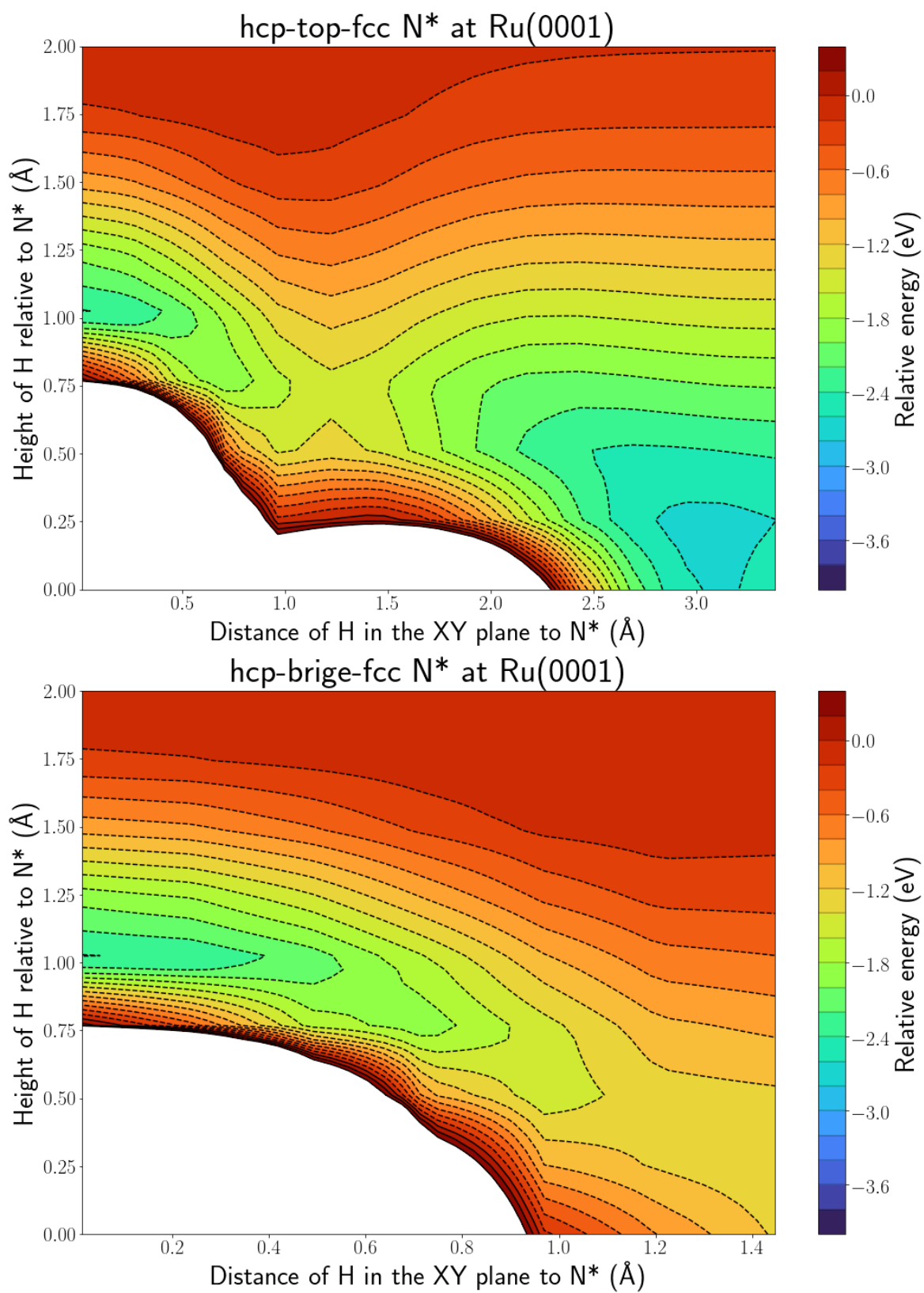


Figure S.7: PES intersection for H(g) + N* at Ru(0001) surface along the hcp-top-fcc line (top panel) and the hcp-bridge-fcc line (bottom panel).

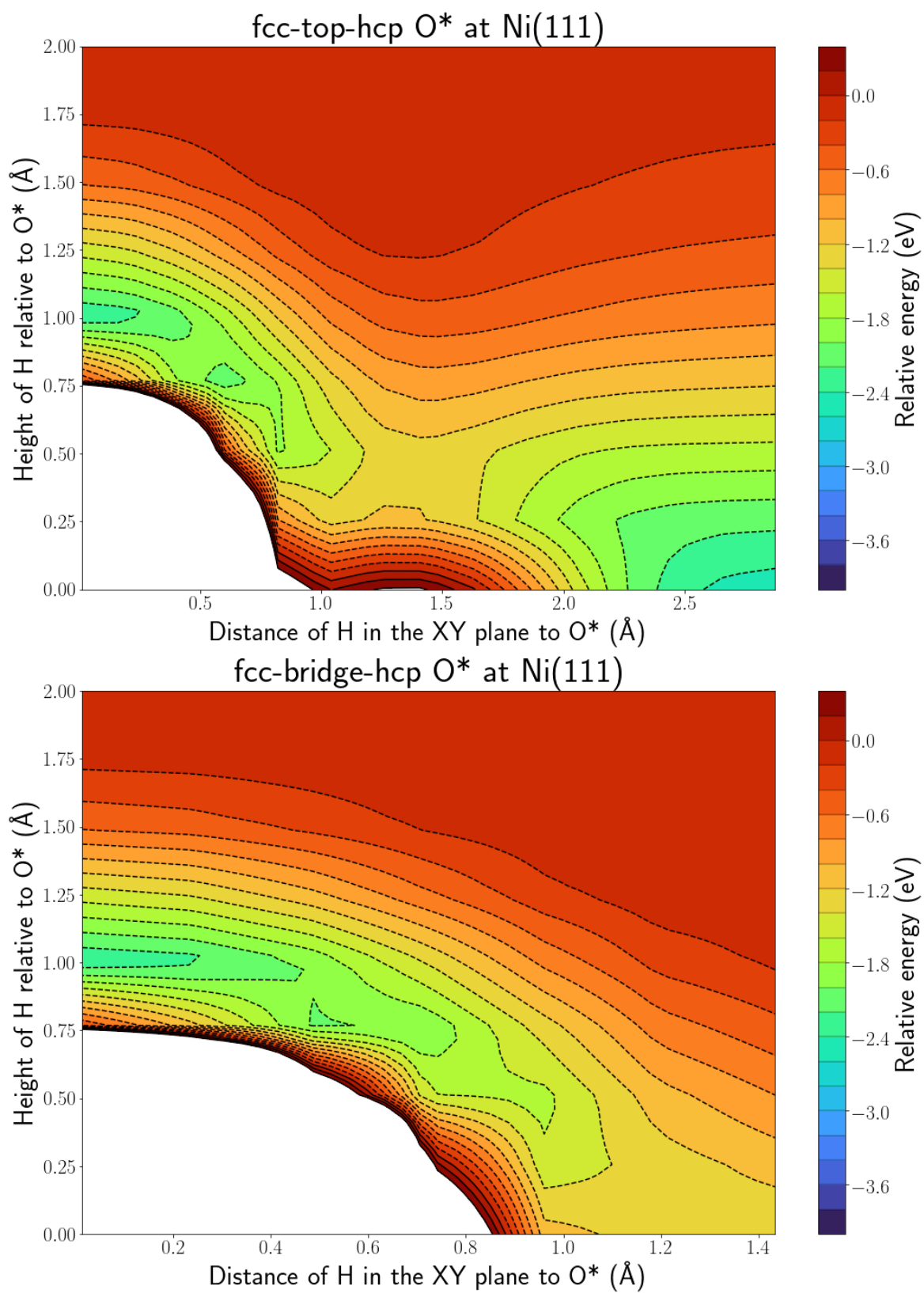


Figure S.8: PES intersection for H(g) + O* at Ni(111) surface along the fcc-top-hcp line (top panel) and the fcc-bridge-hcp line (bottom panel).

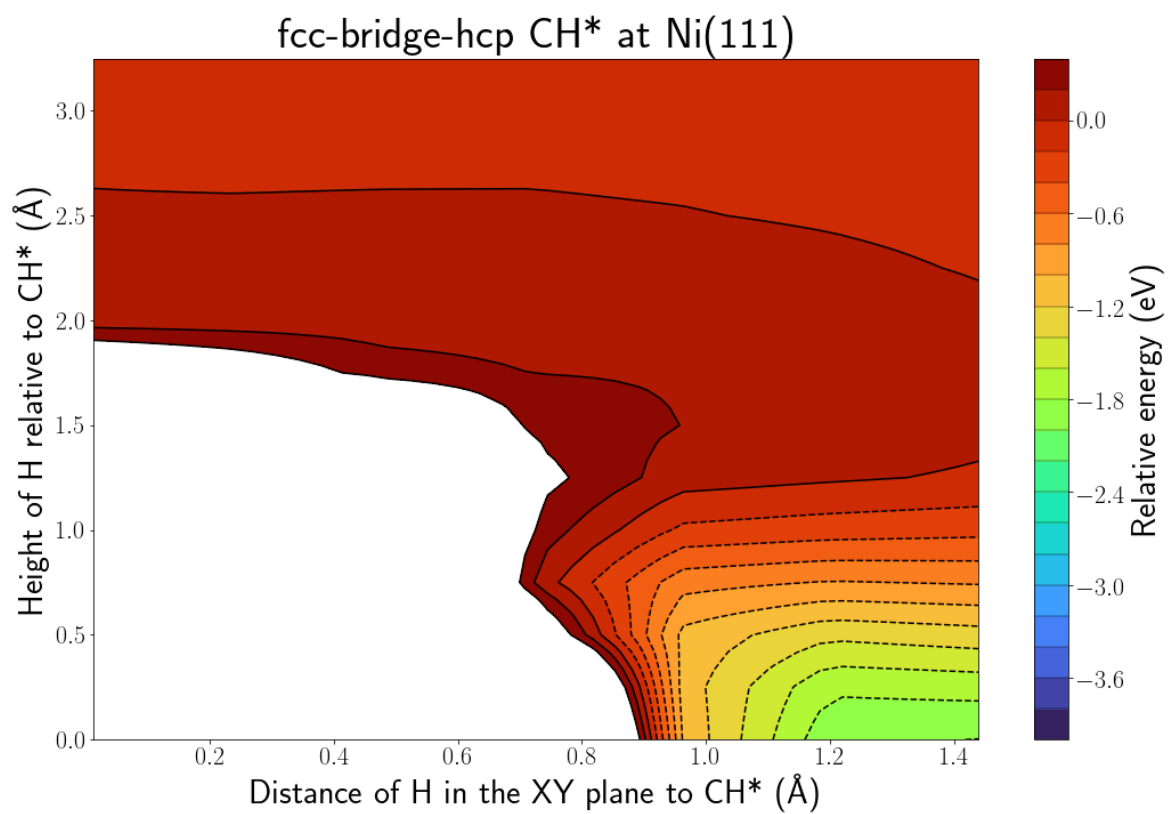


Figure S.9: PES intersection for H(g) + CH* at Ni(111) surface along the fcc-bridge-hcp line.

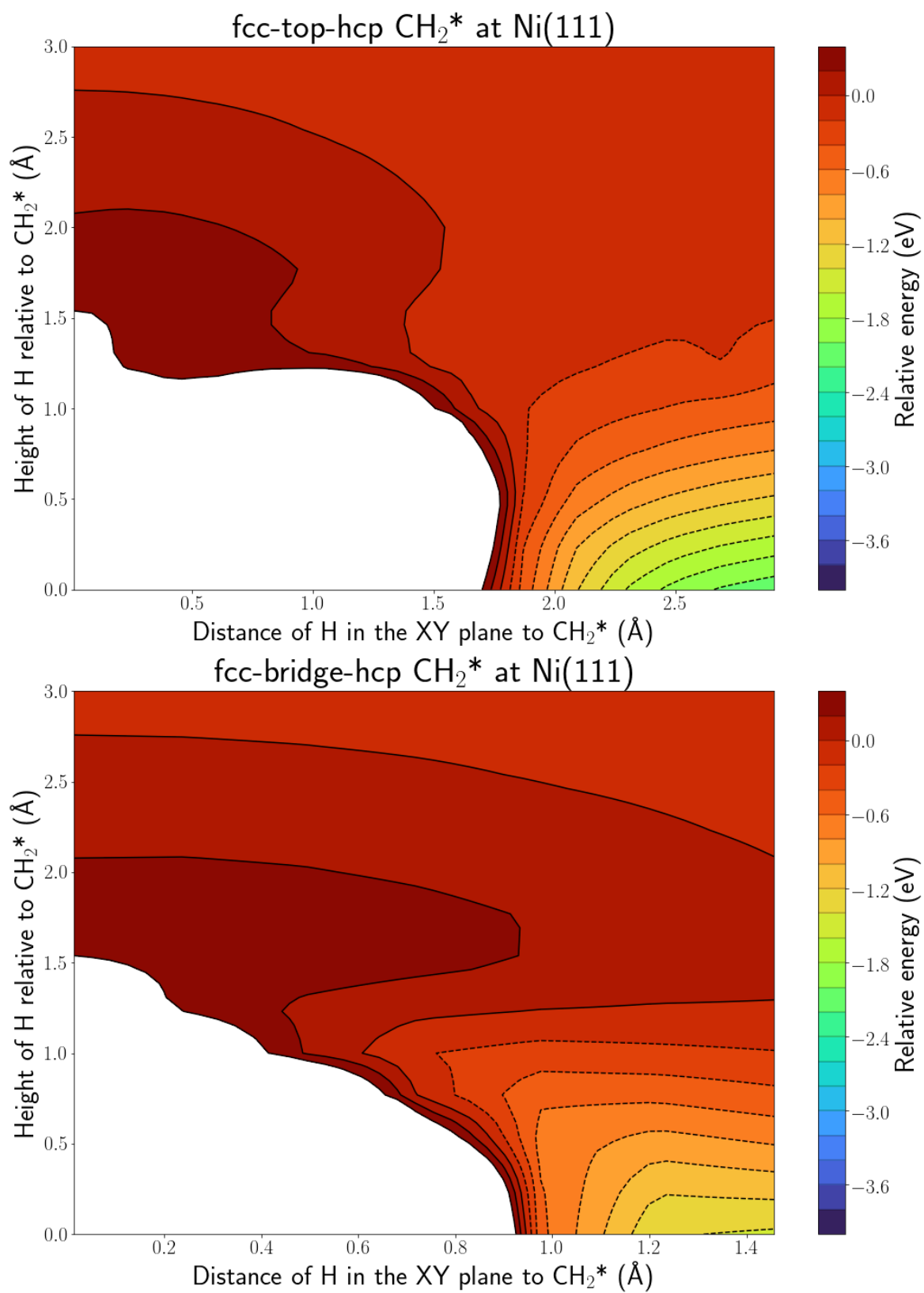


Figure S.10: PES intersection for $\text{H}(\text{g}) + \text{CH}_2^*$ at Ni(111) surface along the fcc-top-hcp line (top panel) and fcc-bridge-hcp (bottom panel).

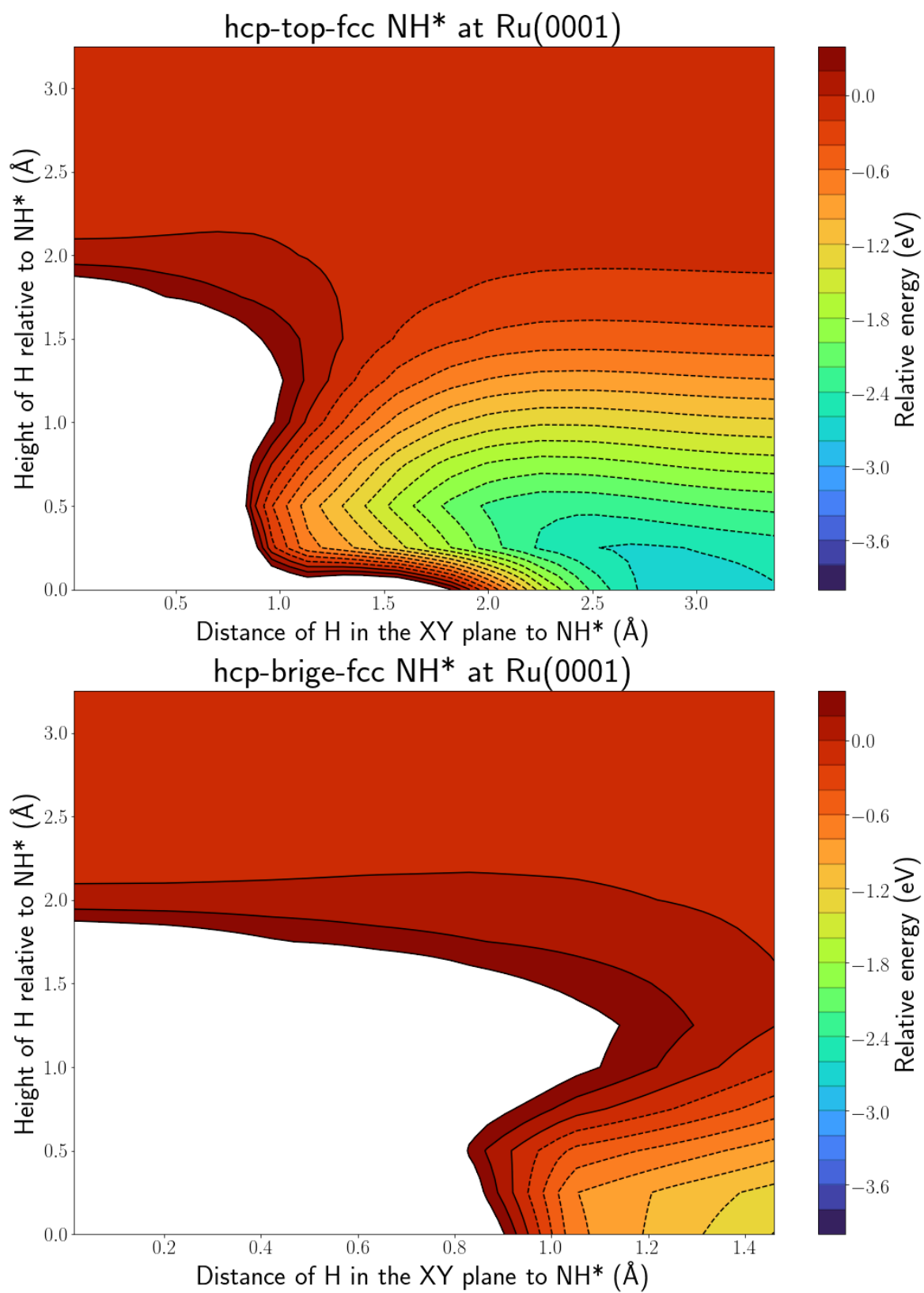


Figure S.11: PES intersection for $\text{H}(\text{g}) + \text{NH}^*$ at Ru(0001) surface along the hcp-top-fcc line (top panel) and the hcp-bridge-fcc line (bottom panel).

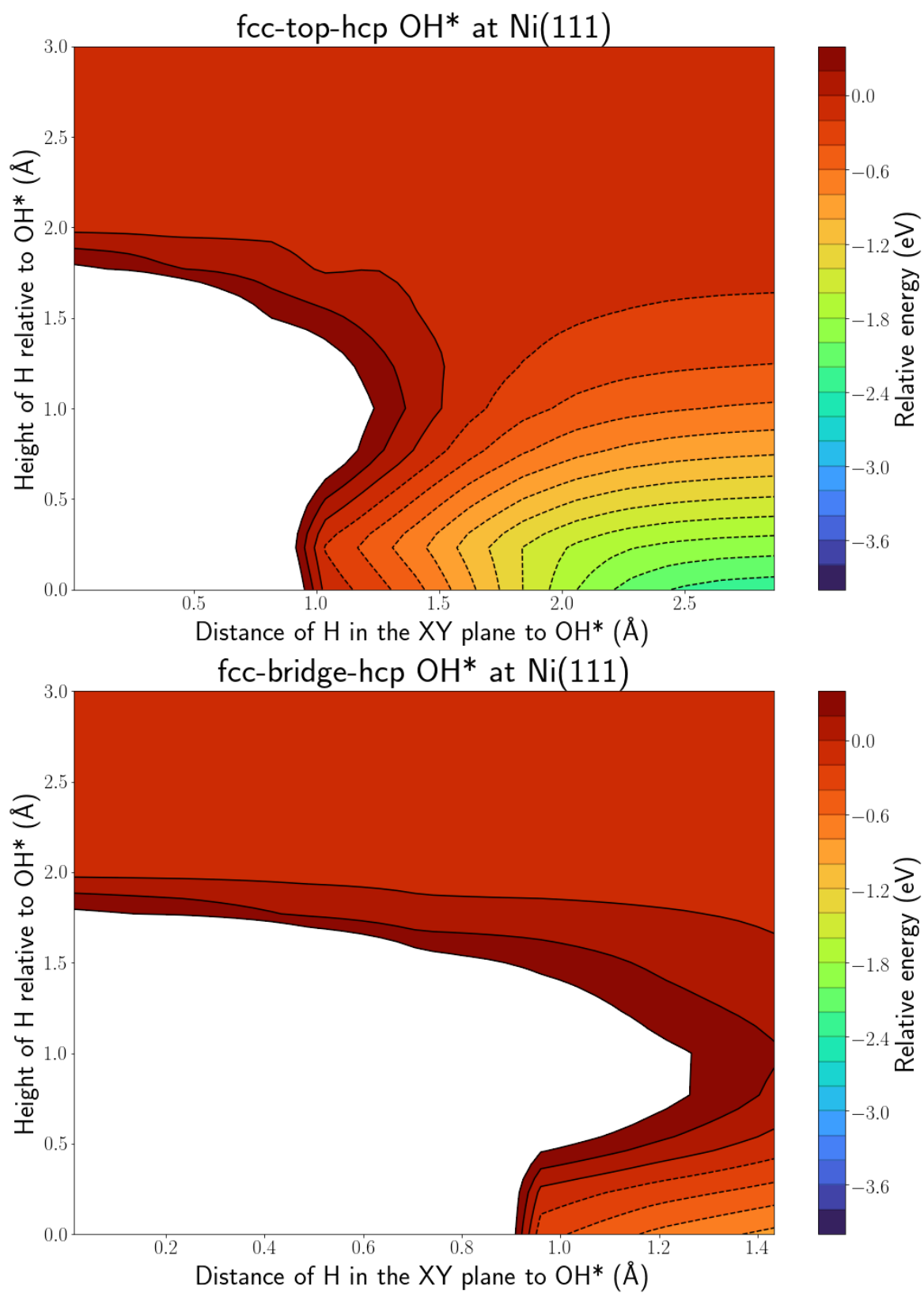


Figure S.12: PES intersection for H(g) + OH* at Ni(111) surface along the fcc-top-hcp line (top panel) and the fcc-bridge-hcp line (bottom panel).

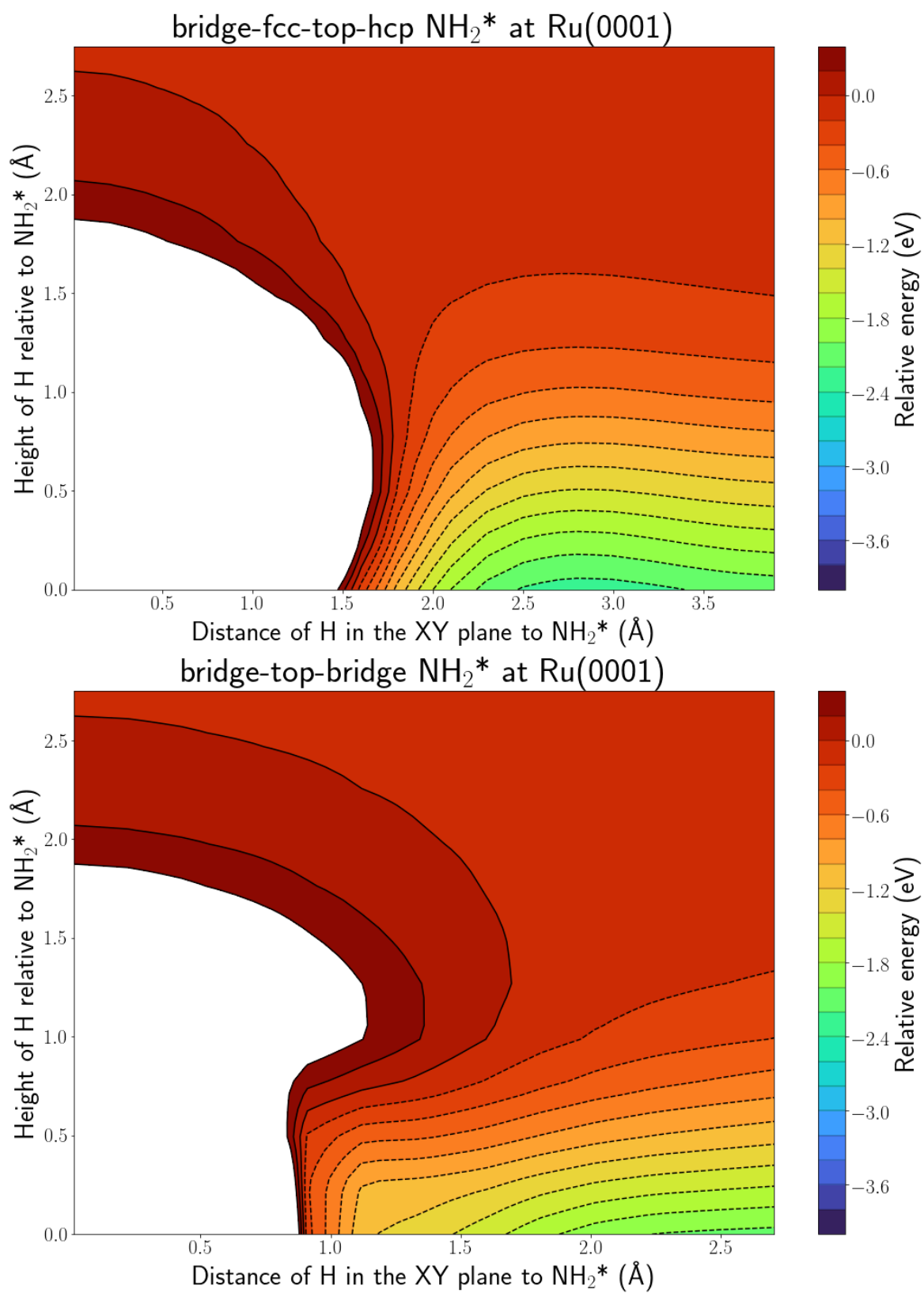


Figure S.13: PES intersection for $\text{H}(\text{g}) + \text{NH}_2^*$ at Ru(0001) surface along the bridge-fcc-top-hcp line (top panel) and the bridge-top-bridge line (bottom panel).

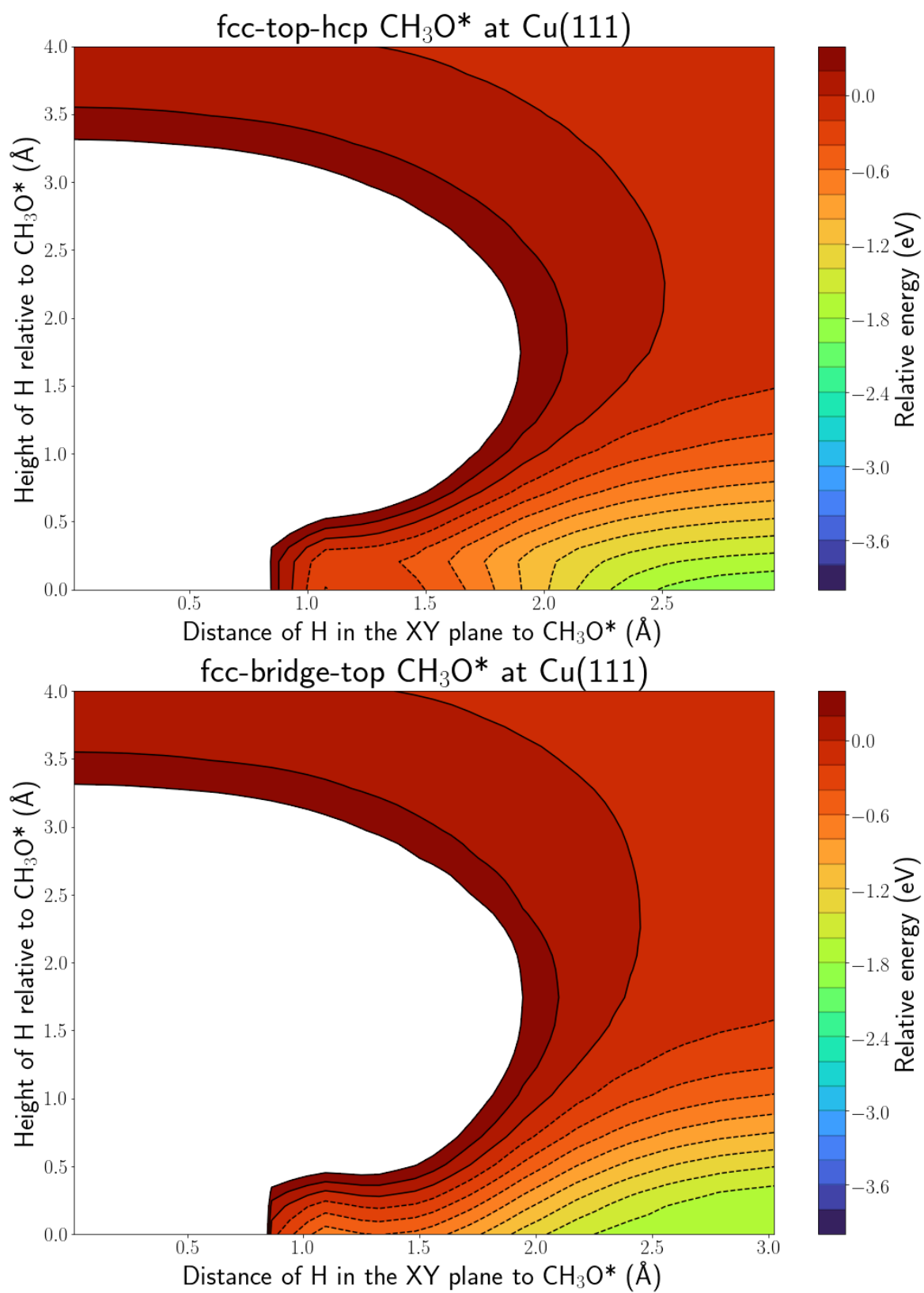


Figure S.14: PES intersection for $\text{H}(\text{g}) + \text{CH}_3\text{O}^*$ at Cu(111) surface along the fcc-top-hcp line (top panel) and the fcc-bridge-top line (bottom panel).

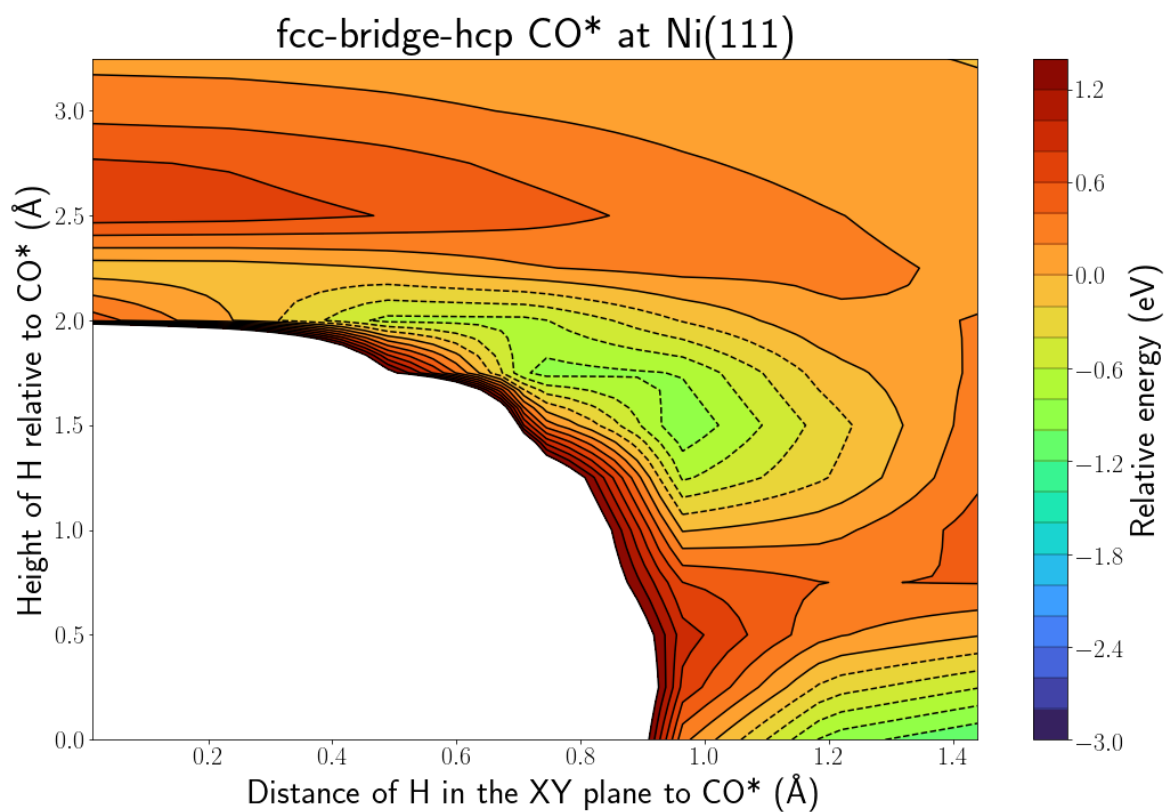


Figure S.15: PES intersection for H(g) + CO* at Ni(111) surface along the fcc-bridge-hcp line.

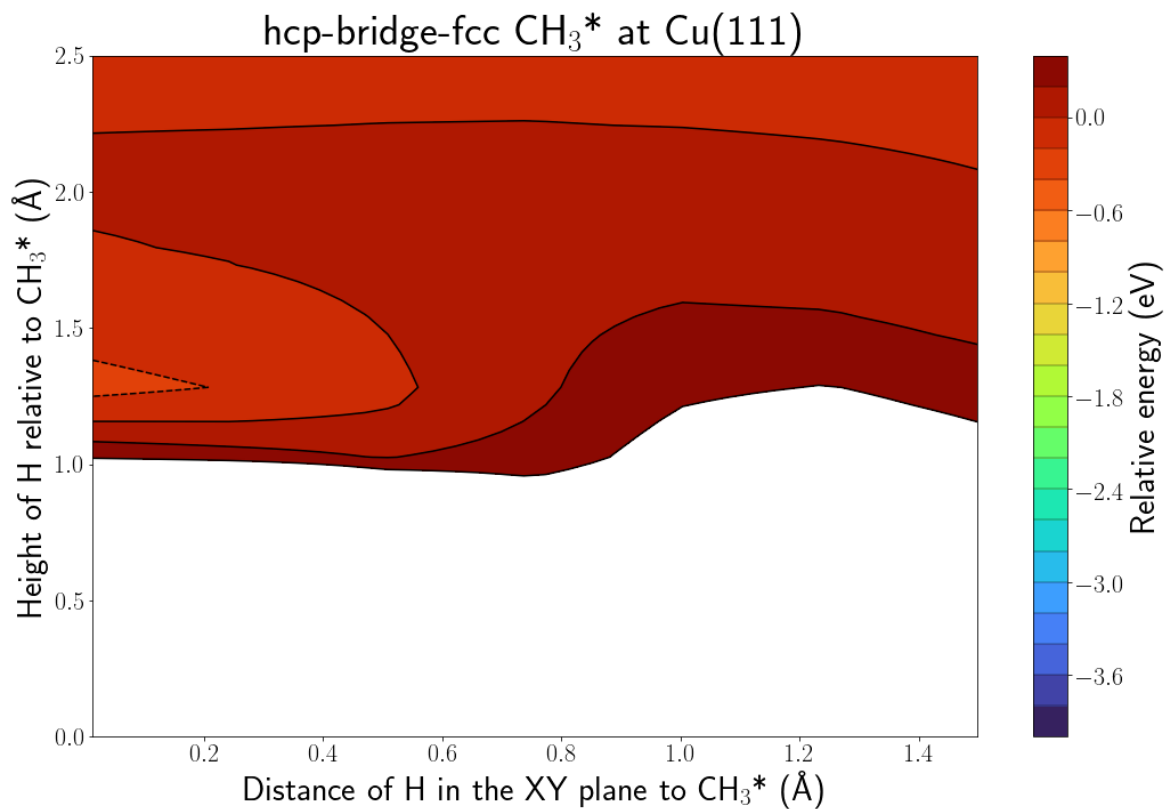


Figure S.16: PES intersection for H(g) + CH₃* at Cu(111) surface along the hcp-bridge-fcc line.

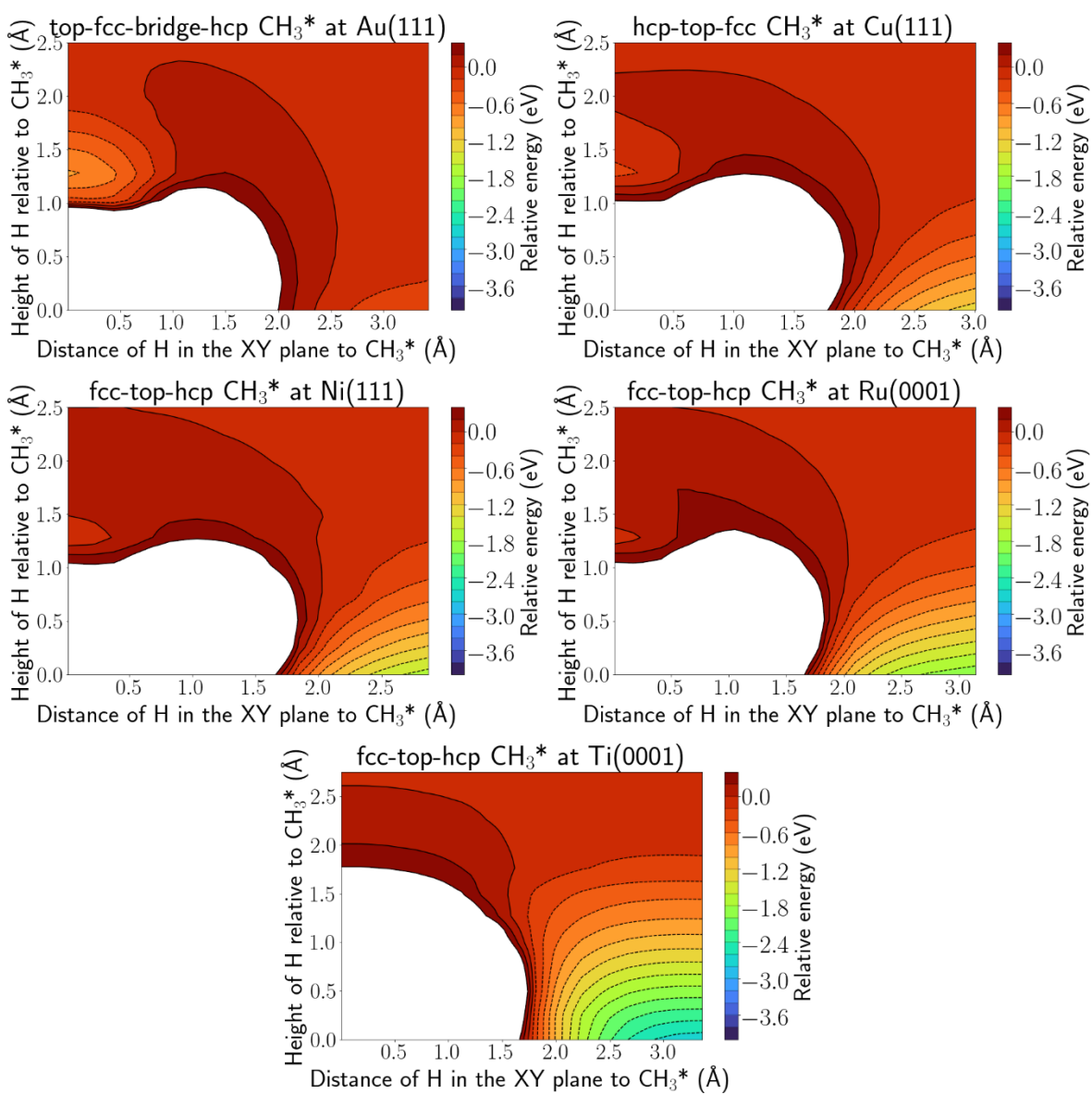


Figure S.17: PES intersection for H(g) + CH₃* at Au(111) (top left), Cu(111) (top right), Ni(111) (middle left), Ru(0001) (middle right) and Ti(0001) (bottom panel).

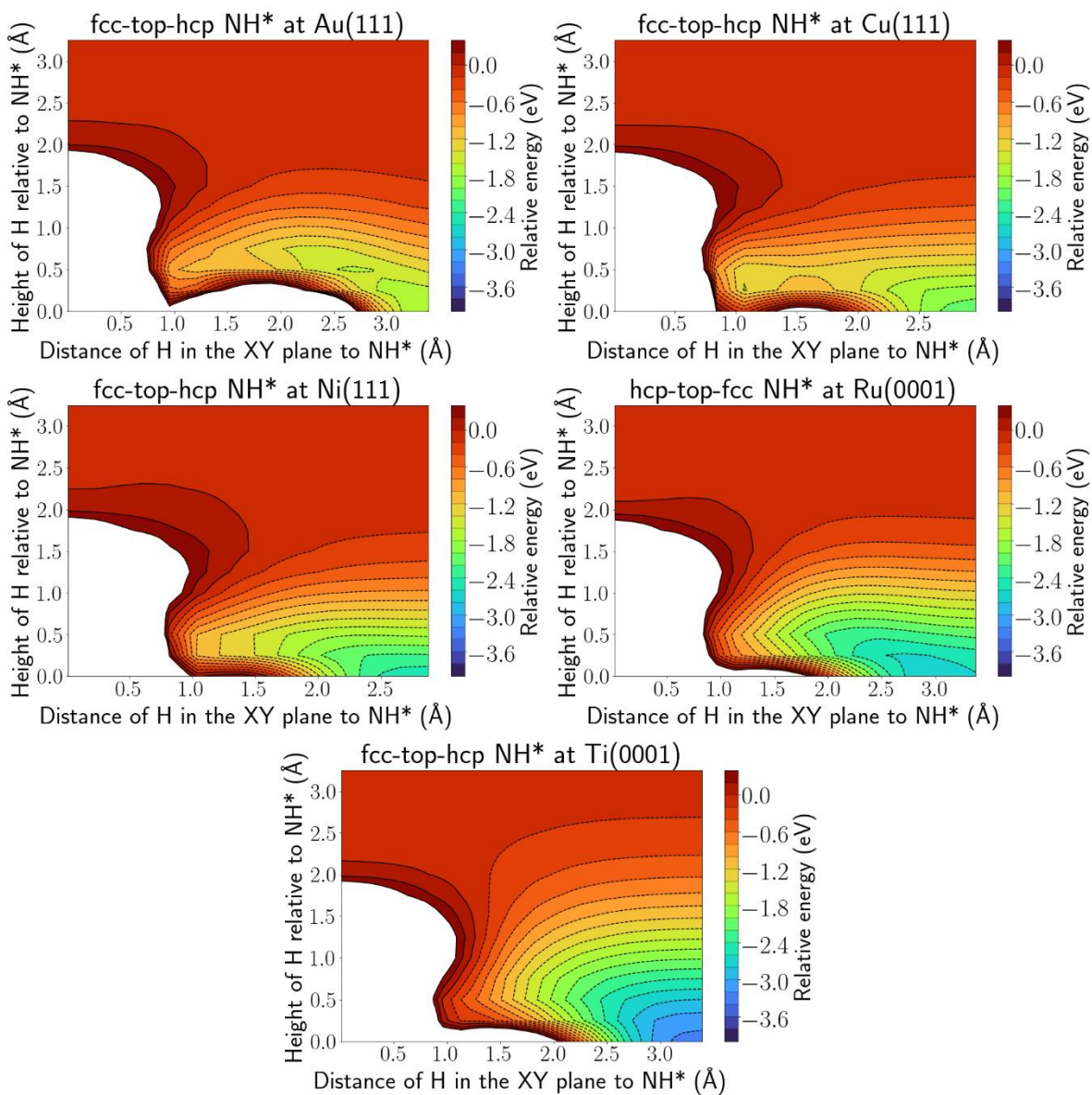


Figure S.18: PES intersection for H(g) + NH* at Au(111) (top left), Cu(111) (top right), Ni(111) (middle left), Ru(0001) (middle right) and Ti(0001) (bottom panel).

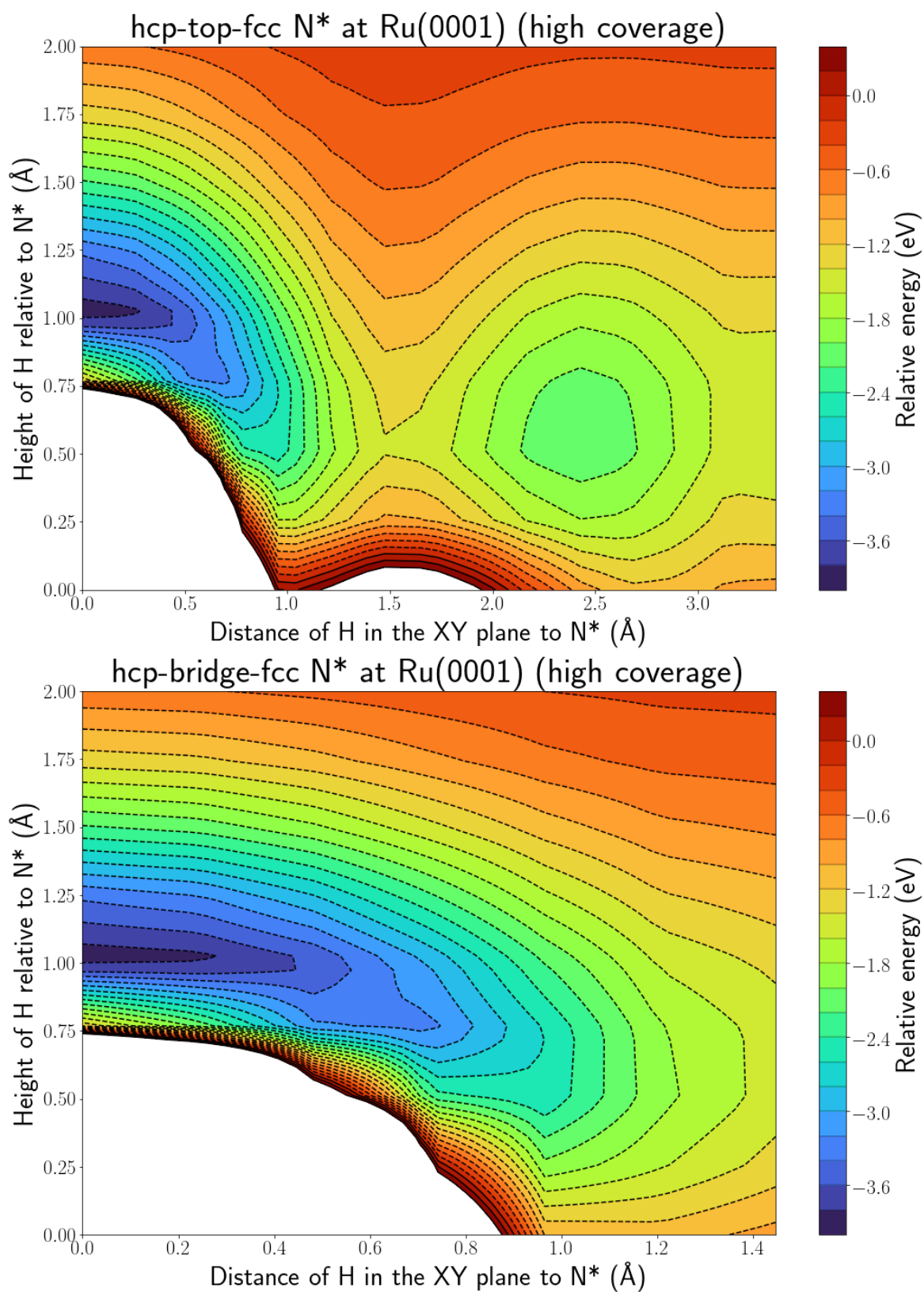


Figure S.19: PES intersection for H(g) + N* at Ru(0001) surface along the hcp-top-fcc line (top panel) and hcp-bridge-fcc line (bottom panel) for a high coverage of N.

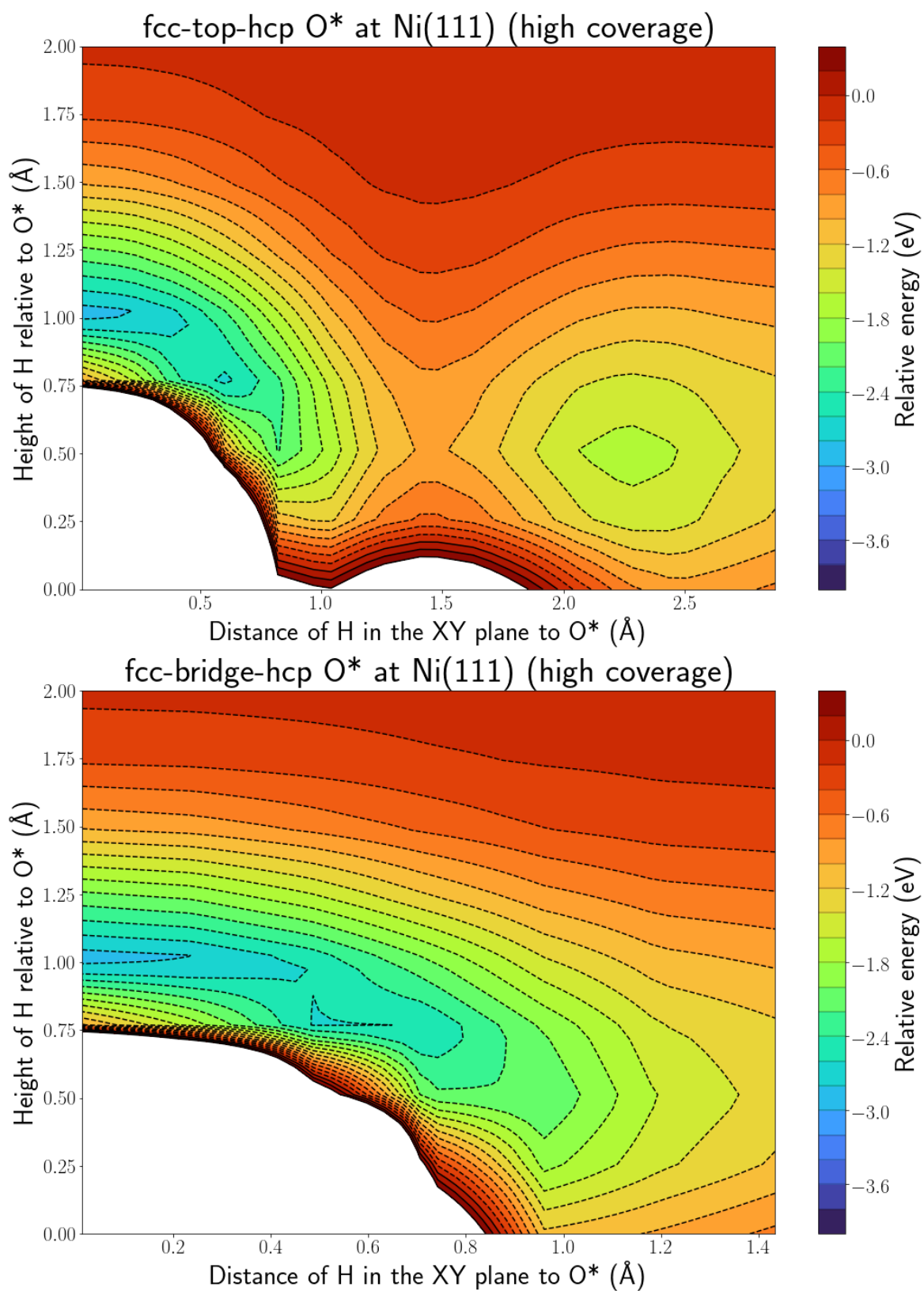


Figure S.20: PES intersection for H(g) + O* at Ni(111) surface for high O* coverage along the fcc-top-hcp line (top panel) and the fcc-bridge-hcp line (bottom panel).

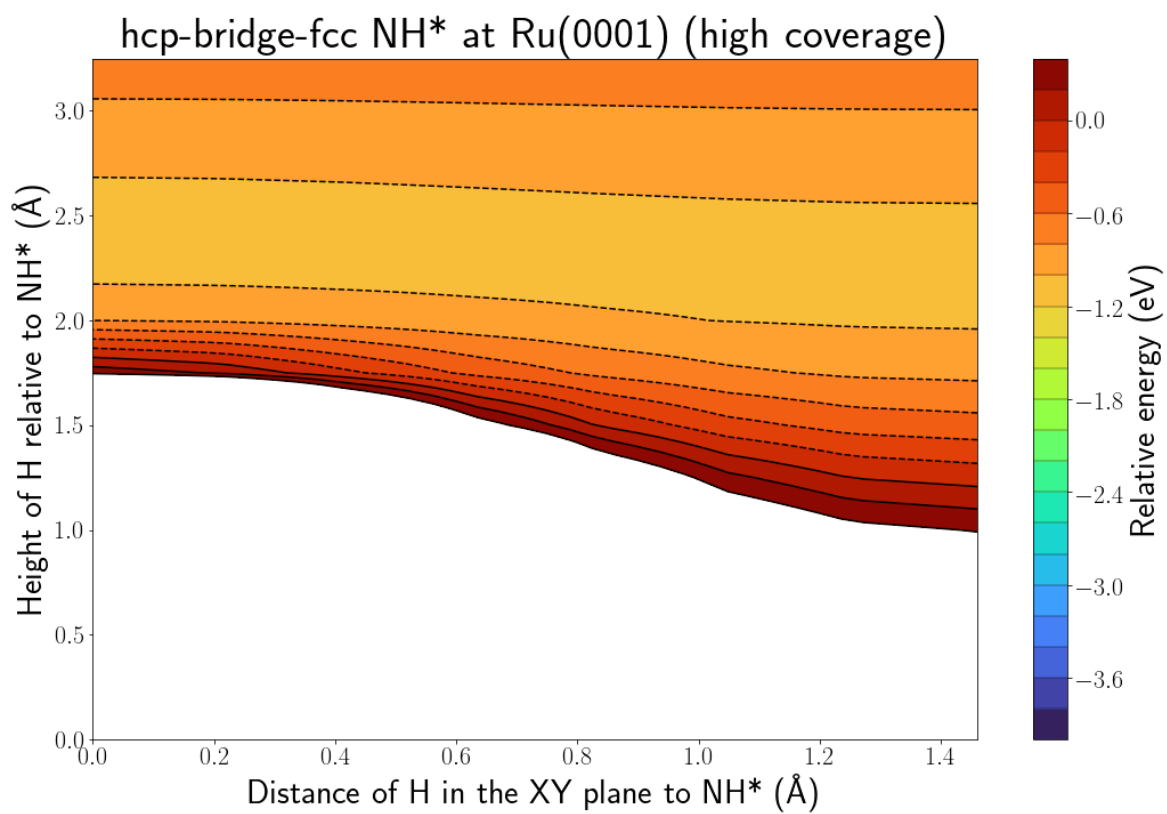


Figure S.21: PES intersection for H(g) + NH* at Ru(0001) surface along the hcp-bridge-fcc line for a high coverage of NH*.

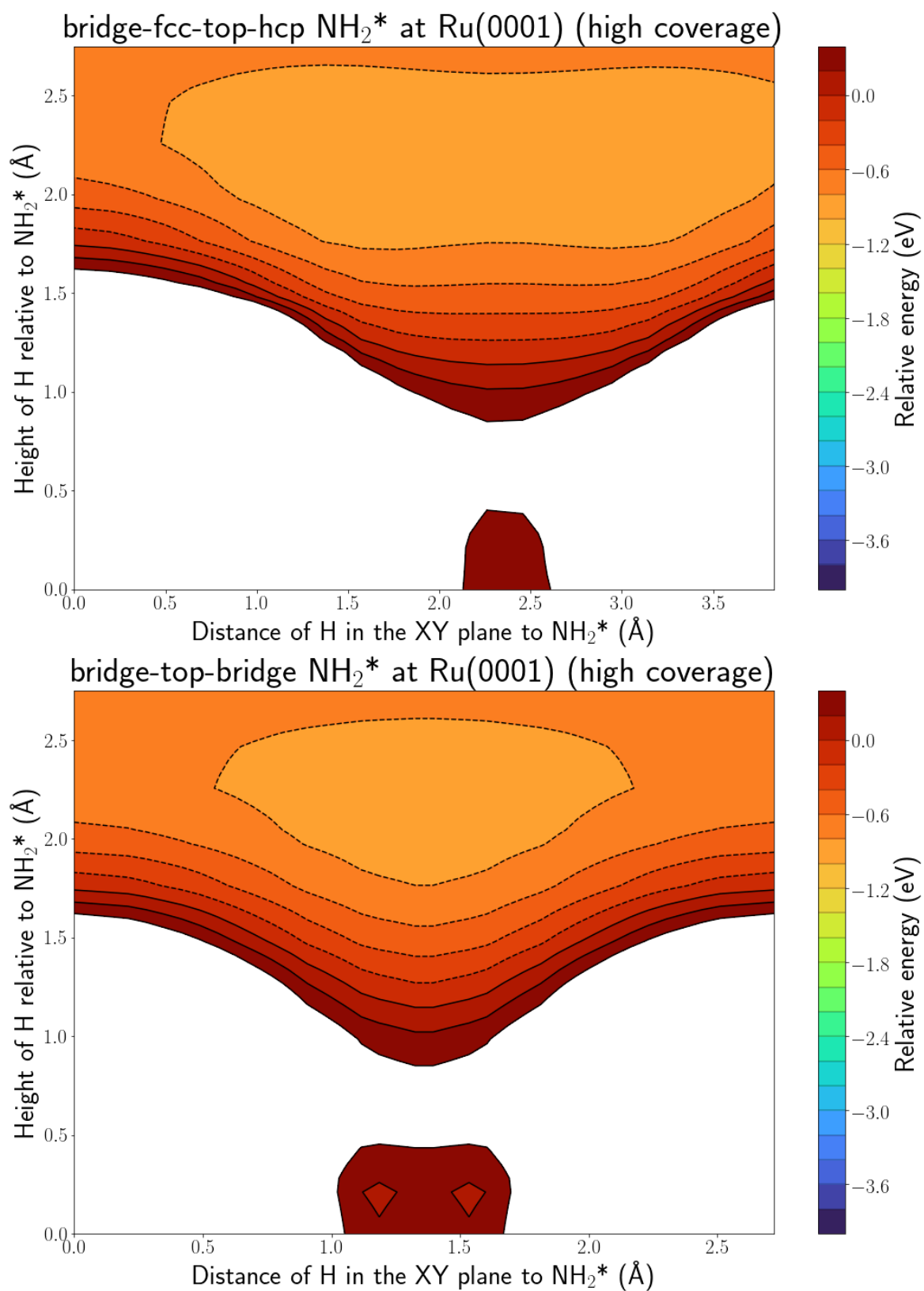


Figure S.22: PES intersection for $\text{H}(\text{g}) + \text{NH}_2^*$ at Ru(0001) surface along the bridge-fcc-top-hcp line (top panel) and the bridge-top-bridge line (bottom panel).

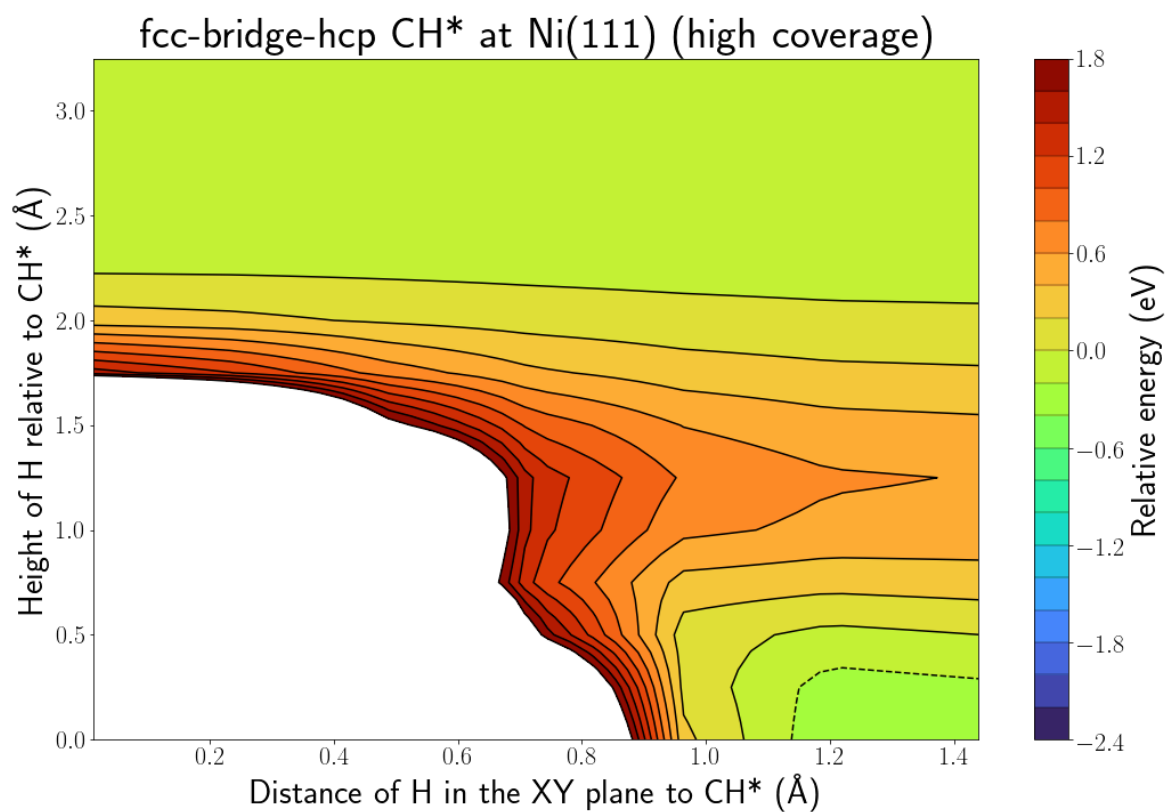


Figure S.23: PES intersection for H(g) + CH* at Ni(111) surface along the fcc-bridge-hcp line for a high coverage of CH*.

S.3 C adsorption energy

Table S.1: C adsorption energies in eV for the different metal surfaces.

Metal surface	Adsorption energy C atom (eV)
Au(111)	-3.82
Cu(111)	-4.23
Ni(111)	-6.21
Ru(0001)	-7.20
Ti(0001)	-7.56